ICANS XIV
14th Meeting of the International Collaboration on Advanced Neutron Sources,
Starved Rock Lodge, Utica, Ill, USA
June 14-19, 1998

Heat Deposition in Mercury by 24 GeV Protons

G S. Bauer, H. Spitzer, G. von Holzen and L. Ni and J. Hastings*

Paul Scherrer Institut
CH-5232 Villigen-PSI, Switzerland

* Brookhaven National Laboratory
Upton, N. Y. 11973, USA

Abstract

The spatial distribution of the power deposited in a Mercury target by 24 GeV protons was measured in order to be able to validate computer codes used in liquid metal target design by comparing computed stress levels on a liquid metal target container to experimental data. After correcting for the measured deviation of the beam position from the target axis, the measured integral power deposition was found to be 57% of the total beam power, in good agreement with theoretical expectations. This gives confidence in the measured spatial distribution which was found to be rather narrower in axial direction than originally anticipated. The results of this experiment are an important input information for the prediction of pressure waves that arise as a consequence of pulsed power input at high power density.

1. Introduction

One important goal of the ASTE (AGS Spallation Target Experiment) Collaboration [1] is to verify experimentally the predictions with respect to power deposition and pressure wave buildup resulting from a short pulse of high energy content (see e.g. [2], [3]). The present report is on the first experimental run in this collaboration, carried out at the Alternating Gradient Synchrotorn (AGS) in Brookhaven National Laboratory in June 1997. Its purpose is to show the viability of the technique selected and to provide a basis for further theoretical and experimental investigations.

2. Parameterization of the Power Distribution in a Spallation Target

The axial distribution of the power deposition by energetic particles in condensed matter (and hence the temperature distribution after a short pulse) has been found to be described rather well by a parameterization of the form [4]:

$$P(z) = P_0 (1-\exp(-(z-z_0)/\lambda_b))*\exp(-z/\lambda_a). \quad (1)$$

Keywords: Mercury, Power deposition, temperature distribution, pressure waves

The following meaning can be attributed to the individual parameters:
λ_a - attenuation mean free path, λ_b - buildup mean free path, z_0 - extrapolation length (giving the distance in front of the target where the analytic curve crosses zero), P_0 - scaling parameter which must be chosen in the right magnitude and units to give the correct integral of the curve.

Eq. (1) can be used to describe the lateral integral or the maximum of the power deposition along the axis, with properly selected parameters. In order to take into account the radial distribution, equ. (1) must be multiplied with the normalized radial distribution function W(r). The most commonly used analytical expressions for the beam profile are a parabolic distribution or a Gaussian. In this case:

$$W(r) = 2/(\pi r_s^2)*(1-(r/r_s)^2) \qquad (2a)$$

for a parabolic distribution of base width r_s or

$$W(r) = 1/(2\pi\sigma^2)*\exp(-r^2/2\sigma^2) \qquad (2b)$$

for a Gaussian with standard deviation σ.

(If the beam profile has elliptic rather than axial symmetry, eqs. (2a) and (2b) must be modified accordingly.) Most of the theoretical calculations have been performed [2], [3] for these distributions. In view of the situation found with the present experiments, a triangular distribution is also considered which, in the general case, is described by an elliptical cone. The normalized radial distribution function W(x,y) in the target geometry coordinate system (x,y) then reads:

$$W(x,y) = 1-\{ [(x-x_0)/A]^2 + [(y-y_0)/B]^2 \}^{0.5} \qquad (2c)$$

where (x_0,y_0) is the center point of the elliptic cross-section of the proton beam with a semi-major axis A and a semi-minor axis B.

In practice the beam will widen as it penetrates into the material. This can be taken into account by allowing r_s, σ, or A and B to become functions of z:

$r_s = r_s(z)$ (3a) $\sigma = \sigma(z)$ (3b) $A = A(z), B = B(z)$ (3c)

3. Experiment

A 20 cm diameter, 1.2 m long cylindrical stainless steel container with a hemispherical front cap filled with Mercury [5] was used as a spallation target in the experiment. In order to measure the spatial power distribution in the target, an array of 32 thermocouples was placed in the lower half-midplane of the cylinder. The 1.5 mm thick encapsulated Chromel - Alumel thermocouples (type K) were thinned down to 0.5 mm over the last 15 mm in order to improve their time response. The positions of the thermocouple tips inside the target are shown in Fig. 1. They were chosen on the basis of an assumed parabolic radial power distribution with a base width of r_s = 5 cm.

A 32 channel Hewlett Packard fast data logging system was used to scan the thermocouple readings every 15 ms over a period of 30 sec and to record the readings on disk. The length of the cables between the thermocouples and the data logger was 50 m. The noise corresponded to

roughly 0.5 K, in agreement with the specifications given by the manufacturer. Data recording was triggered from a pulse derived from a beam monitor.

For the beam intensity and profile measurement, an Al foil, 20x20 cm^2, 25 μm thick was placed on the beam axis in front of the target near the exit of the beam pipe by the JAERI group[6].

4. Experimental results

4.1 Proton beam profile

The distribution of the proton induced ^{22}Na and ^{7}Be activity was determined by placing the foil on an image plate and integrating the measured radioactivity over pixel sizes of 2x2 mm^2. Fig. 2 shows the resulting intensity distribution for the Al foil. The coordinate system chosen is a right handed system with z along the direction of the proton beam and y in the vertical direction. It can be seen that the beam cross section is roughly elliptic. The beam center is not located in the target coordinate center. The coordinates of the beam axis are $x=x_0$, $y=y_0$. A beam profile with fitted parameters is schematically shown in Fig. 3. The parameters used are (cf section 3.4)

$$(x_0, y_0) = (-0.5 \text{ cm}, -1.0 \text{ cm}) \qquad A = 8.5 \text{ cm} \qquad B = 6 \text{ cm} \tag{4}$$

4.2 Temperature data evaluation procedure

Useful thermal data could only be collected during run 22 in which, according to the information obtained from the AGS control room, two bunches of 24 GeV protons with $4*10^{12}$ particles per bunch were injected into the target. All other runs were of significantly lower power and did not produce useful signals on the thermocouples.

Examples of the thermocouple recordings over the full period of 30 seconds are shown in Fig. 4 for the thermocouples 1 and 2 (located at distances z of 30 and 80 mm from the apex of the hemispherical cap on the axis of the target). Polynomial trend lines were fitted to the measured data using the corresponding feature of EXCEL. Such trend lines (without the original data, for clarity) are also shown for the thermocouples Nr. 7, 20 and 28 for illustration. The initial rise of these trend lines is an artifact resulting from the first (low) data points and should not be taken seriously.

A few striking features are immediately obvious from Fig. 4: The rapid power dissipation over only 10 seconds and a bump for thermocouple Nr.1 after 15 seconds. These will be discussed below in section 3.3.

For the quantitative evaluation of the temperature distribution in the whole target, polynomial fits were applied to the readings of all thermocouples for the first 5 seconds after the pulse. Examples are shown in Fig. 5. The values of the fitted curves at t = 500 ms were taken as representing the maximum temperatures reached and were plotted as a function of position of the thermocouples in Fig.6. The lines are guides to the eye only.

4.3 Temperature dissipation in the target

After the proton pulse the temperature appears to stay more or less constant for almost 1 sec and then starts to drop rapidly. This drop must be attributed to the onset of convection because it cannot be explained in terms of the thermal conductivity of Hg. Calculations of the heat dissipation by conduction alone give a much slower temperature decrease (Fig 7), indicating that it would take minutes for the temperature to return to the original value. By contrast, the measured temperatures are back to their equilibrium values (22.4 °C in Figs. 4 and 5) within less than 25 seconds. This clearly indicates the importance of convection in the system.

The other prominent feature in Fig. 4 is the temperature rise for TC Nr. 1 that starts some 13 seconds after the pulse. Although this still needs to be checked in detail, one possible explanation might be that this is a consequence of the convective motion in combination with the hemispherical shape of the target front cap: Warm liquid rising to the top might have been circulating along the wall of the front cap to replace the liquid moving up from the hot region and might have reached the front most thermocouple before fully cooling down. If this effect is reproduced in future measurements, we will perform suitably detailed calculations to investigate it more closely.

4.4 Lateral distribution of the power deposition

Since the beam maximum was not on the target axis, the maximum of the temperature distribution was not sensed by the thermocouples. The following procedure was adopted to determine the fraction of the total power sensed by the thermocouples from the measured beam distribution:

An indication to the direction of the displacement can be obtained from the neutron leakage distribution measured on four positions of the target periphery [7], albeit on a different 24 GeV run, as shown in Fig. 8. Since the top left detectors recorded the highest intensity, it seems likely that this was the direction of the displacement of the beam axis relative to the target axis. In order to verify this, the measured beam intensity distributions along $x = 0$ and $y = 0$ were plotted in Figs 9a and 9b as a function of position (top scales) and were compared to the temperatures recorded for the thermocouples of the first row (at $z = 80$ mm). Since no thermocouples closer to the beam monitor foil were available, the readings at $z = 80$ mm were taken as representing the temperature measurement for $x = 0$, $y > 0$, $z = 0$. The same thermocouple readings are plotted in all four symmetry planes in order to facilitate the comparison with the beam profile data. Clearly, there is good correspondence of the temperature readings only with one curve, which must, therefore, represent the lower half plane ($x = 0$, $y > 0$). This confirms that the beam profile was displaced to the top left as shown in Fig. 3, where the projection of the plane of the thermocouples is also indicated. From this the assignment of the positive and negative signs to the half axes in x and y follows unambiguously as shown in the bottom scales of Figs. 9a and b. This assignment is also in agreement with the measured neutron distribution (Fig. 3)

The beam profile can be approximated fairly well by an elliptical cone with its peak at (x_0,y_0). This cone was used to fix the parameters given in section 3.1 for an analytical approximation to the beam profile. The triangle shaped intersection curves with the planes $\{x=x_0, y\}$ respectively

{x, $y=y_0$} (symmetry planes of the beam coordinate system) are shown in Figs. 9a and 9b by the symbols. The intersections of the cones with the respective symmetry planes of the target coordinate system (hyperbolae) are shown by the solid lines. These curves are to be compared to the measured beam intensities along the axes x = 0 and y = 0. Although, in this representation, the fit curves seem to more or less envelope the measured data, the beam integrals under the measured values and the cone used for the fit agree to within 0.13%.

4.5 Axial distribution of the temperature rise

In Fig. 10 the squares show the axial distribution obtained from collecting the maximum thermocouple readings along the axis of the target, together with a fit according to equ.1 for T instead of P (solid line)

The parameters of the fit for x = 0, y = 0 are:

Parameter	λ_a	λ_b	z_0	T_0	
Fit to experiment	18 cm	8.5 cm	-1.2 cm	7.9 °C	(5)

Since the measured distribution was not along the beam axis but along x = 0 , y = 0 (projection plane in Fig. 3), the temperatures on the beam axis were obtained by extrapolation of the measured values to $x = x_0$, $y = y_0$: The dashed line represents this extrapolation to the beam axis, as discussed below.

4.6 Axial distribution of the lateral power integral.

In order to estimate the total power dissipation in the target, a spatial distribution of the temperature field had to be constructed from the measured values. This requires extrapolation to regions downstream of the volume in which thermocouples were located, using the values of the measured minor semi axes at the positions available. The latter are plotted in Fig. 11. The uncertainty in these data rises with increasing z due to the low temperature rise measured. In particular, the value at z = 48 cm should not be taken seriously and has been left out of Fig 11. The values up to z = 38 cm do not warrant anything but a linear fit, although, from a physics point of view, a higher order polynomial would be more appropriate. Therefore, as a lower limit to the actual beam spreading in the target, a linear relation can be used to describe the increase of B(z) as a function of z. The relation

$$B_{l.m} = B + y_0 = 4.512+0.061*z\ [\text{ cm }] \qquad (6a)$$

shown by the thin line in Fig. 11 was fit to the experimental data.

As a probably more realistic description, it is also possible to match the second order relation

$$B_{p,m} = B + y_0 = 4.9+0.0015*z^2 [\text{ cm }] \qquad (6b)$$

to the experimental points, as shown by the heavy solid line in Fig. 11.

Inserting the value of -1 cm found for y_0 yields:

$$B_l(z) = 5.512 + 0.061*z \text{ [cm]} \qquad (7a) \qquad \text{or } B_p(z) = 5.9 + 0.0015\ z^2 \text{ [cm]} \qquad (7b)$$

Since no experimental data were available for the horizontal mid-plane, the corresponding relations for the semi-major axis were derived, assuming the ratio A(z)/B(z) to remain the same as for z = 0 cm, i.e. in the proton beam, throughout the target. This yields:

$$A_l(z) = 7.80867 + 0.08642*z \text{ [cm]} \qquad (8a) \quad \text{or } A_p(z) = 8.3583 + 0.002125*z^2 \text{ [cm]} \qquad (8b)$$

Using the parabolic extrapolation, the full representation of the temperature distribution becomes

$$T(x,y,z) = 9.6*\exp(-z/18)*[1-\exp(-(z+1.2)/8.5)]*(1-\text{sqrt}\{[(x-x_0)/A(z)]^2 + [(y-y_0)/B(z)]^2\}) \qquad (9)$$

with

$$A(z) = 8{,}36+0.0021*z^2 \qquad B(z) = 5.9+0.0015*z^2 \qquad x_0 = -1.0, \qquad y_0 = -0.5$$

which, for x = 0, y = 0 represents the measured data (solid line) and for $x = x_0$, $y = y_0$ yields the dashed curve in Fig. 10.

From this it follows that the maximum temperature rise in the target was 4.08°C, corresponding to a peak power density of 7.66 J/cm^3 (using a value of 0.139 J/gK for the specific heat capacity and 13.52 g/cm^3 for the density of mercury)

The corresponding power density distributions around the beam axis at ($x = x_0$, $y = y_0$) in the y,z and x,z planes respectively are plotted in Figs. 12a and b.

Numeric integration over the whole target volume of the power distribution determined in this way yields the total power deposition as listed in Table 1. The values per proton are based on $8*10^{12}$ p/pulse.

Table 1 *Results for the energy deposition in the Mercury target for 24 GeV protons*

Radial extrapolation	Total energy per pulse	Total energy per proton	% of beam power
linear	16.7 kJ	13 GeV	54.4
parabolic	18.7kJ	14.6 GeV	60.9

5. Discussion and Conclusions

In summary, the overall spatial dependence of the power density (J/cm^3) was found to be reasonably well described by the relations

$$p(x,y,z) = P(z)*(1-\{ [(x-x_0)/A]^2 + [(y-y_0)/B]^2 \}^{0.5}) \quad (10a)$$

with P(z) being the power deposited along the center line perpendicular to the elliptic beam at (x_0, y_0):

$$P(z) = P_0 \{1-\exp(-(z+1,2)/8,5)\}*\exp(-z/18) \quad (10b)$$

and with

$$A_p(z) = 8.3583 + 0.002125*z^2 \text{ [cm]} \quad (10c)$$

and

$$B_p(z) = 5.9 + 0.0015*z^2 \text{ [cm]} \quad (10d)$$

The parameter P_0 was determined as 18.05 for 24 GeV protons on Mercury.

The fact that, while the analytical expression for the beam profile used matches the measured integral to within 0.13% (section 3.4), but more or less envelopes the measured data in the main peak area means that the total power deposition is probably represented correctly, but the peak power density is somewhat overestimated. In terms of using this distribution for the stress wave calculations this means that the results will be on the high, i.e, conservative side.

The power integral for the parabolic extrapolation of A(z) and B(z) yields a total of 18.7 kJ, or 60.9% of the total beam energy which is in the same range as those usually found at lower beam energies.
In view of the large uncertainty associated with several of the input data, no attempt was made to establish the confidence level of the results obtained. Nevertheless, it is comforting to see that the data lie well within what is also found at lower proton energies. Since the neutron source distribution is intimately connected with the power density distribution, this shows that, if available, even 24 GeV protons are likely to make a decent spallation neutron source.

In any case, this preliminary experiment clearly showed that a set of thermocouples can be used to determine the power deposition in the Mercury target at the pulse levels available at the AGS. It also became obvious, how important information on the beam profile and position is, in order to be able to evaluate the data properly. Although the Al-foil technique seems to have worked well in the present situation, a second method (wire scanner, giving digital readings directly) as foreseen for future runs will be of great value. Also, the possibility of steering the beam on the target and of measuring with more precision the total number of protons actually hitting the target will be indispensable in determining the confidence level of the experimental results.

While calculations on the stress levels expected on the basis of the current power deposition are in progress, it can be anticipated that the data obtained from future measurements will form a better

basis to compare measured strain data with calculated stress levels and to provide valuable input for the nuclear and CFD-design of the targets and heat removal systems of future spallation neutron sources. Measurements at lower beam energies and more than two bunches per pulse seem, therefore, highly desirable.

6. Acknowledgment

This work was carried out within the ASTE collaboration. The authors are grateful to the operations team of the AGS accelerator for their efforts and cooperation in providing the required proton beam in the experimental line used and also to their colleagues within the collaboration for their help and for sharing information needed to carry out the evaluation of the measured data. The work at Brookhaven National Laboratory was supported by the U. S., Department of Energy under Contract DE-AC02-98-CH10886 with Brookhaven Science Associates.

7. References

[1]G.S. Bauer, J. Hastings and N. Watanabe " Opportunities and Goals of a Spallation Target Test Experiment at the AGS in Brookhaven -The ASTE-Collaboration " in preparation.

[2]K. Skala and G.S. Bauer, "On the Pressure Wave Problem in Liquid Metal Targets for Pulsed Spallation Neutron Sources" Proc. ICANS XIII, PSI-Proceedings 95-02 (1995) pp 559-576

[3]L. Ni and G.S. Bauer "Dynamic Stress of a Liquid Metal Target Container Under Pulsed Heating", submitted for publication to ASME Journal of Pressure Vessel Technology.

[4]G.S. Bauer, H. Sebening, J.-E. Vetter and H. Willax (eds) "Realisierungsstudie zur Spallations-Neutronenquelle" Vol. 1, Report Jül-Spez-113 and KfK 3175 p.75

[5]G:S: Bauer, H. Conrad, P. Martinez and H. Stechemesser, " A Target-Moderaror -Reflcetor System for Spallation Target Test Experiments with Liquid Mercury at the AGS in Brookhaven " in preparation

[6]The JAERI Team, "Measurement of Proton Beam Profile for AGS Target Experiment", Report presented by H. Nakashima, 2nd General ASTE Planning Meeting, Paris, Sept. 25 and 26,1997

[7] The JAERI Neutronics Measurement Group, "Measurement of Reaction Rate Distribution of Activation Detectors on Mercury Target Bombarded with Protons of 1.5, 7 and 24 GeV" Report presented by H. Takada, 2nd General ASTE Planning Meeting, Paris, Sept. 25 and 26,1997

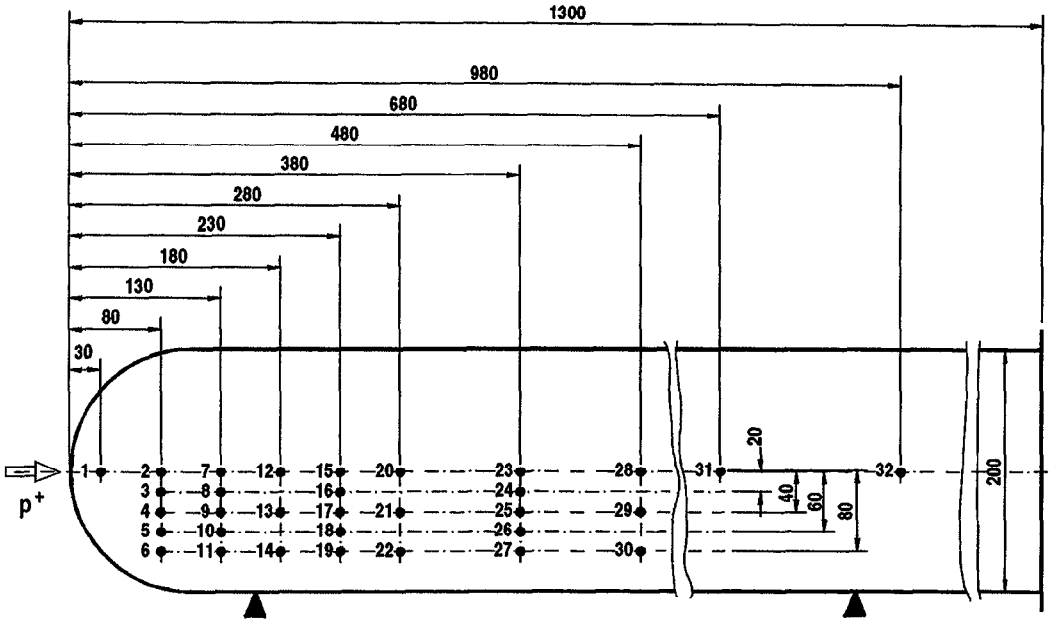

Fig. 1 Positions of the 32 thermocouples in the lower half of the mid-plane inside the target

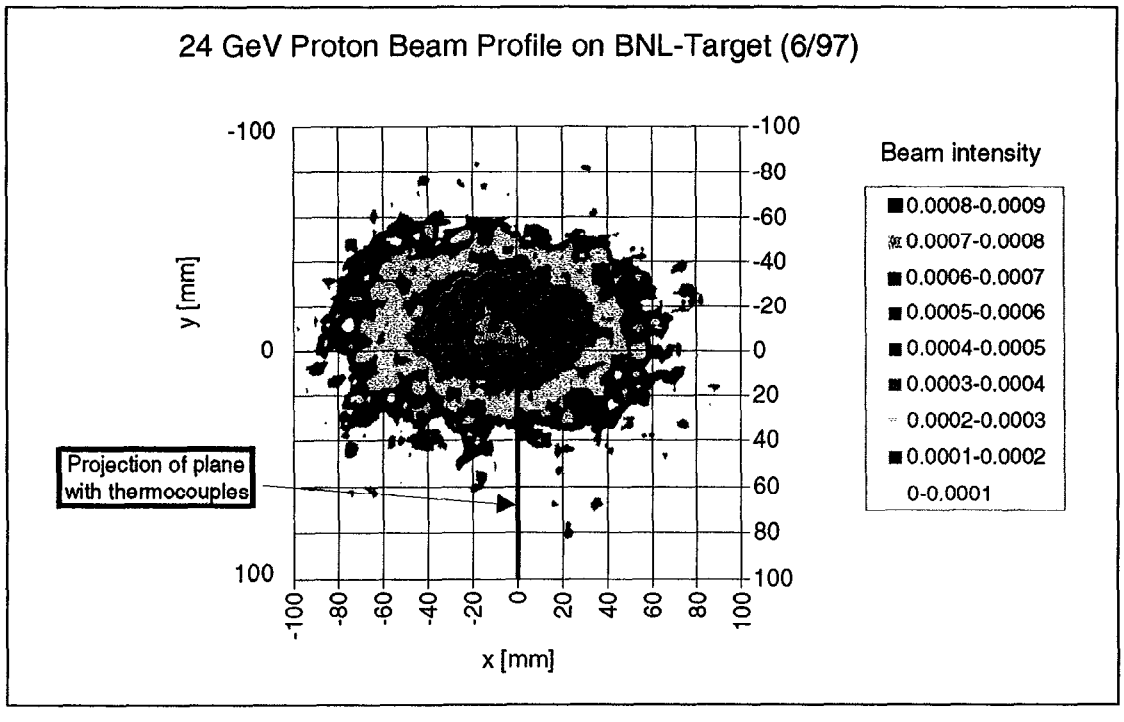

Fig. 2 Measured proton beam profile on the Al foil

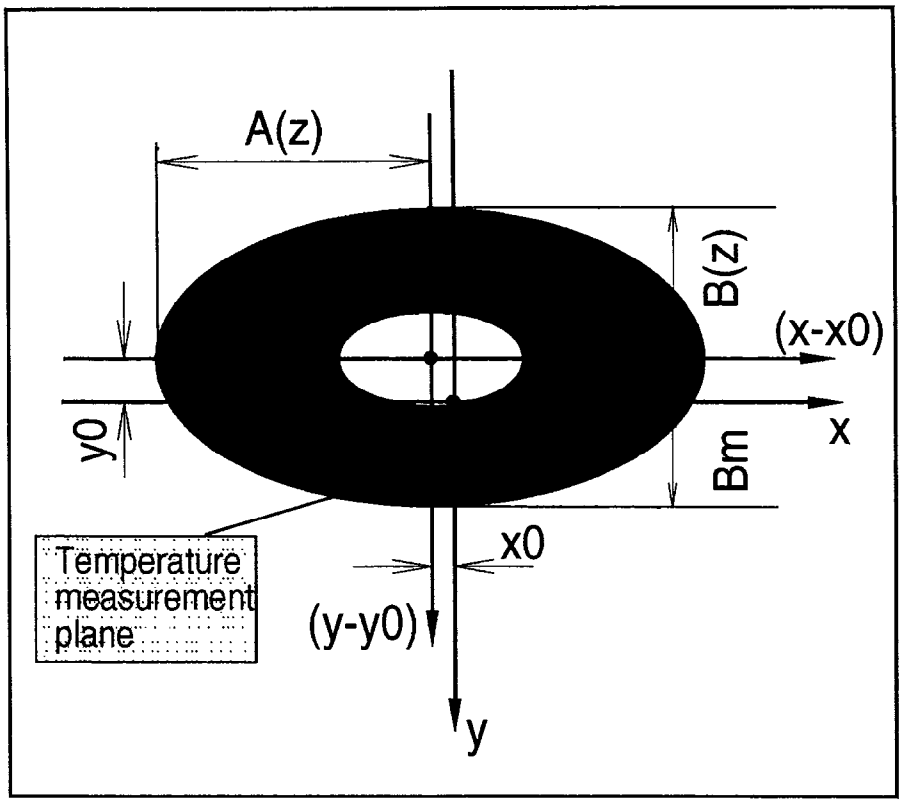

Fig. 3 Nomenclature used for the beam profile

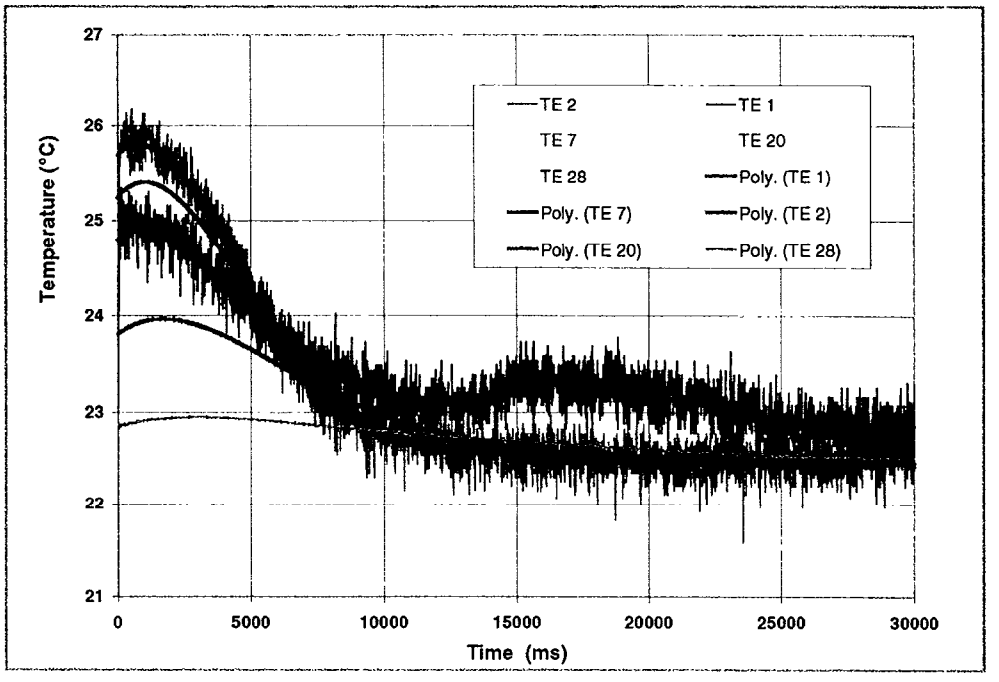

Fig. 4 30 sec temperature evolution for selected on-axis thermocouples

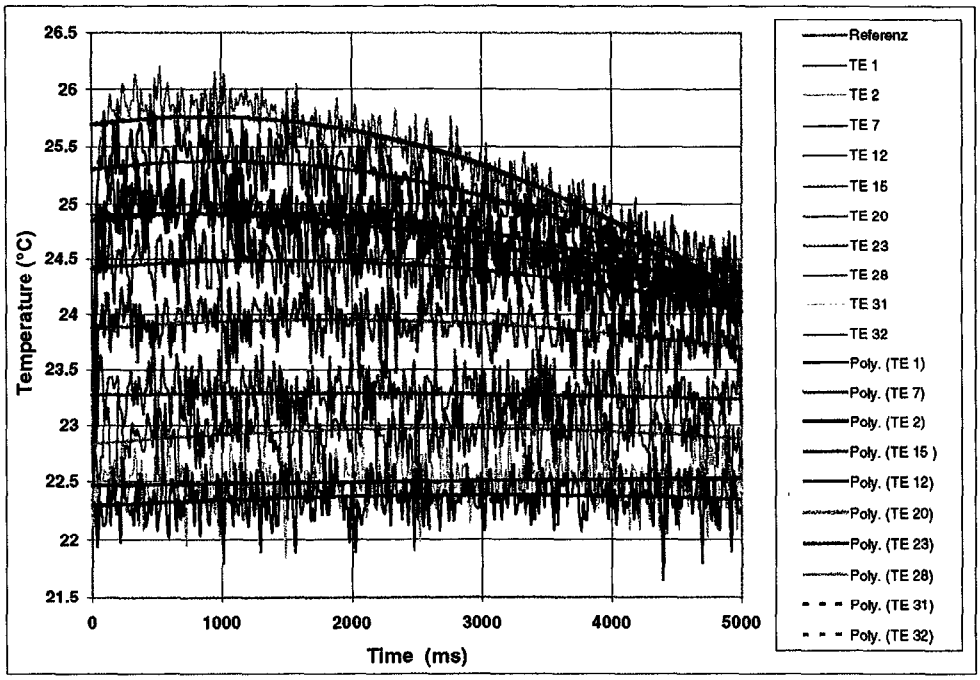

Fig. 5 Temperature histories of the thermocouples for the first 5 seconds

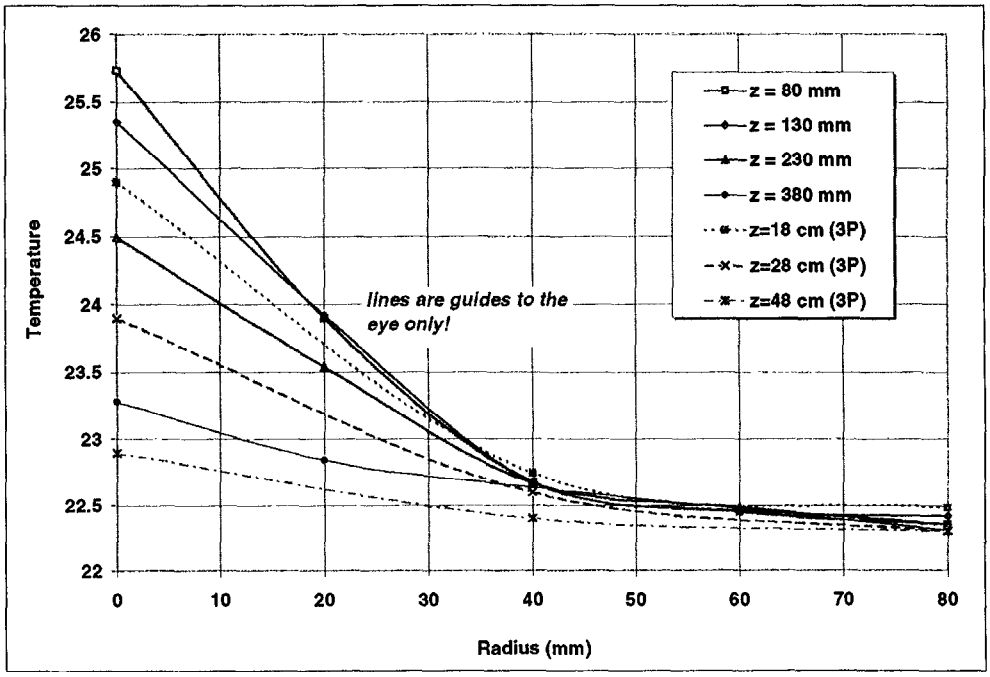

Fig. 6 Radial temperature distribution at various distances z into the target

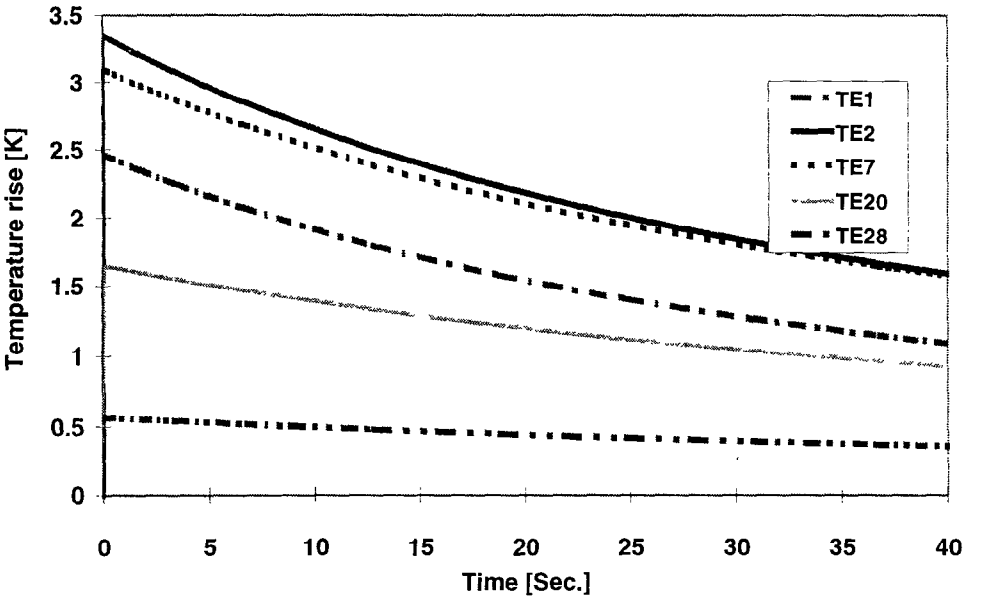

Fig. 7 Calculated temperature evolution for heat dissipation by conduction only

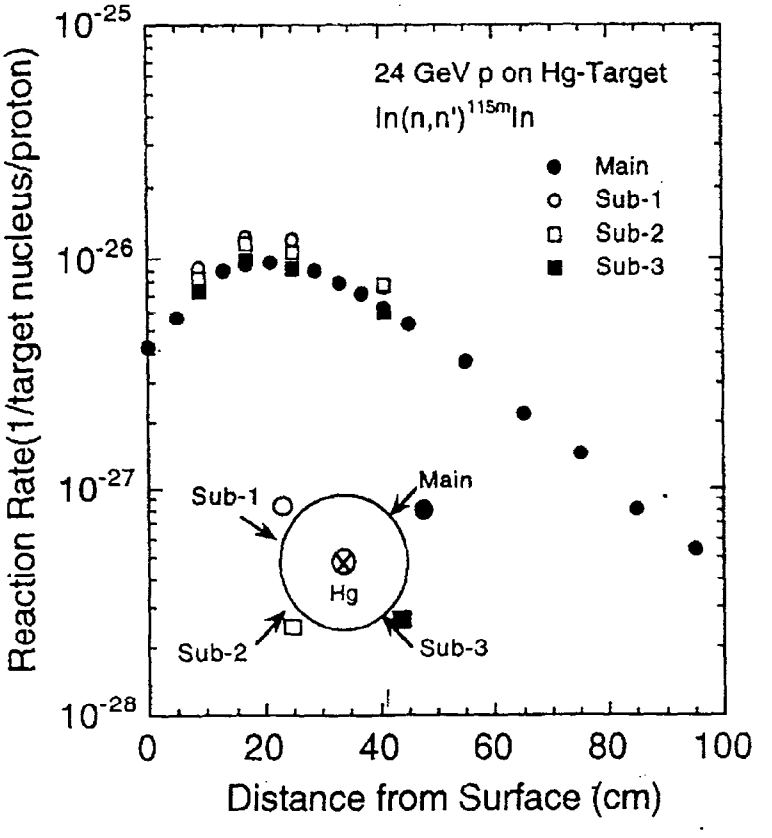

Fig. 8 Reaction rate distribution of $In(n,n)^{115m}$ measured on the cylindrical surface of thick mercury target bombarded with 24GeV protons

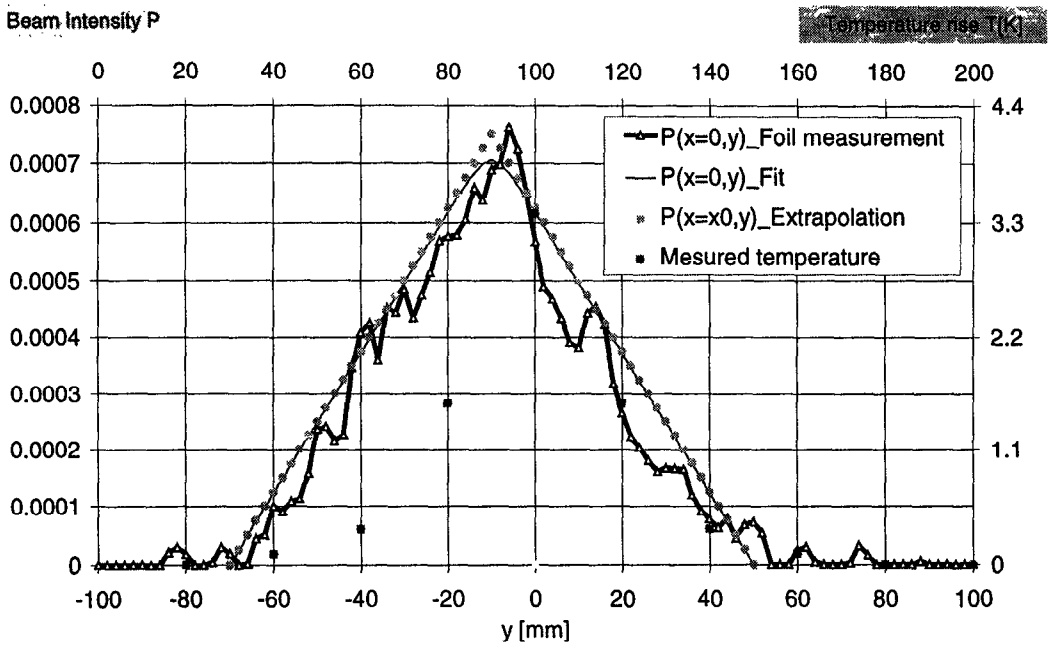

Fig. 9a: Measured and fitted beam distribution along the axes x=0 and $x=x_0$

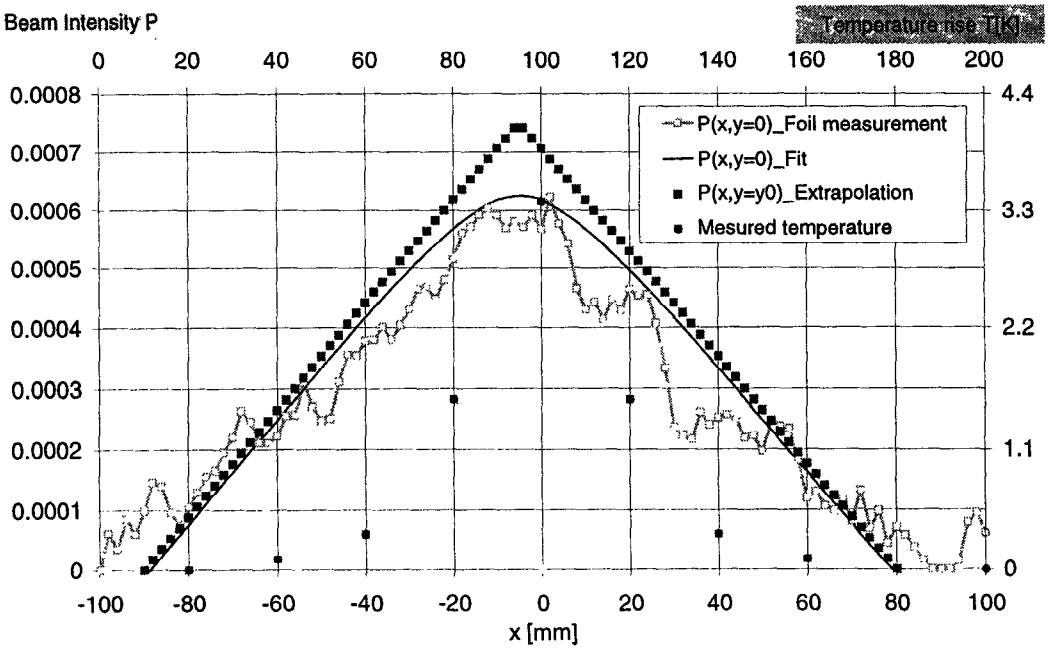

Fig. 9b: Measured and fitted beam distribution along the axes y=0 and $y=y_0$

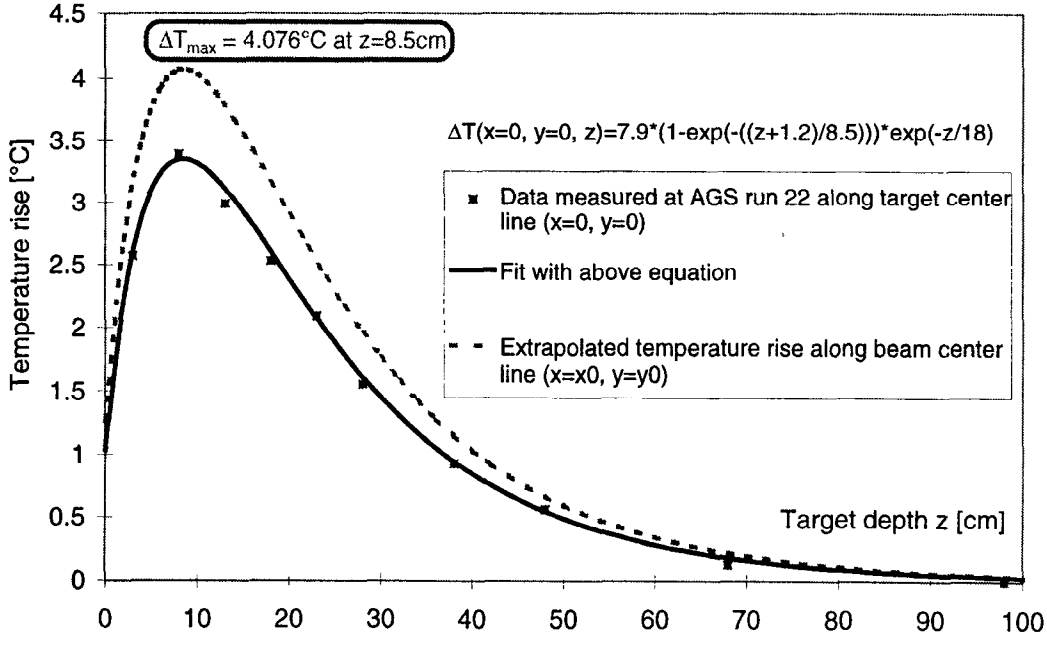

Fig. 10 Measured axial temperature distribution

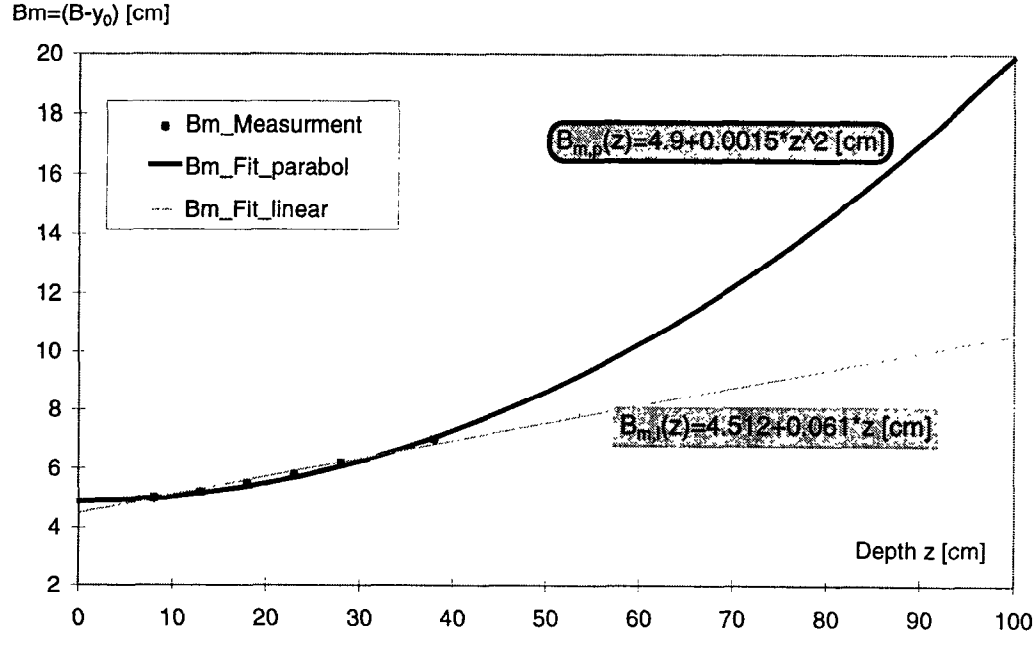

Fig. 11: Fitted semi-minor axes of the elliptic beam

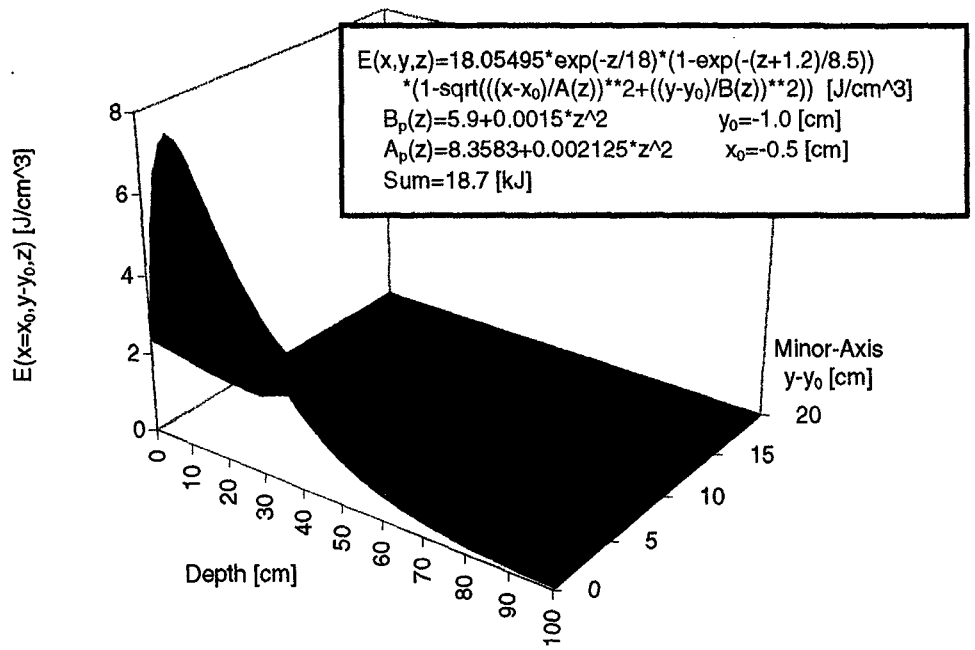

Fig. 12a: Power density distribution along axes $x=x_0$ and z with parabolic fitting

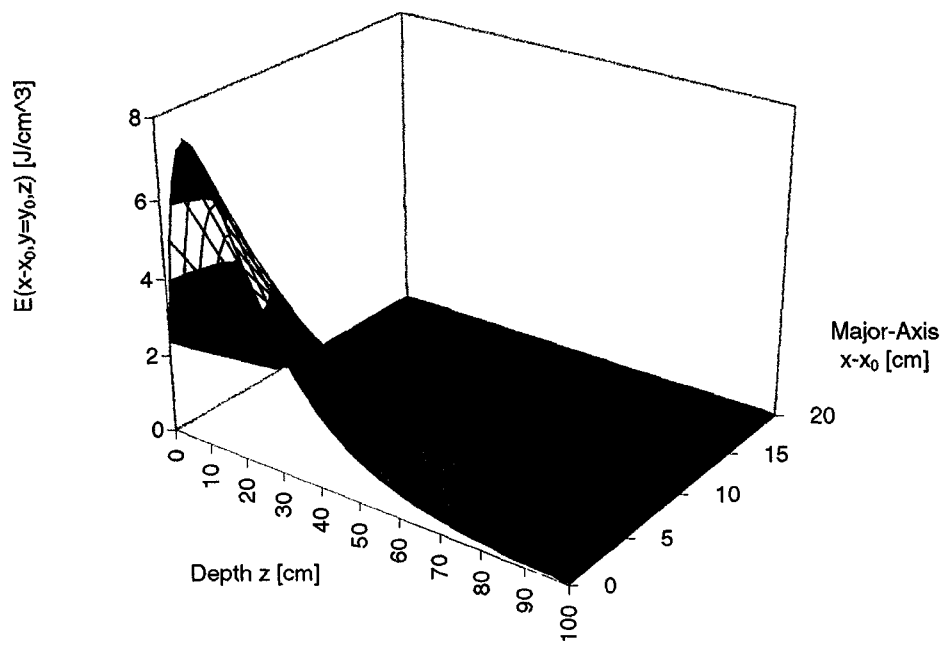

Fig. 12b: Power density distribution along axes $y=y_0$ and z with parabolic fitting